Polarization Forces in Water Deduced from Single Molecule Data

E. V. Tsiper*

School of Computational Sciences, George Mason University, Fairfax, Virginia 22030, USA
Center for Computational Materials Science, Naval Research Laboratory, Washington, D.C. 20375, USA

(Received 8 July 2004; published 13 January 2005)

The intermolecular electrostatic and polarization interactions in water are determined using a minimal atomic multipole model constructed with distributed polarizabilities. Hydrogen bonding and other properties of water-water interactions are reproduced by only three multipoles μ_H, μ_O, and θ_O and two polarizabilities α_O and α_H, which characterize a single water molecule and are deduced from single-molecule data.

DOI: 10.1103/PhysRevLett.94.013204 PACS numbers: 34.20.Gj, 33.15.Kr

Understanding electrostatic and polarization forces is vital in many molecular systems such as molecular clusters, liquids, or solids, specifically those containing polar and polarizable molecules. Polarization effects in water are particularly strong, as can be judged by the enhancement of the molecular dipole from 1.855 D for an isolated molecule to 2.6–3.2 D in condensed state [1,2]. Water is a very fundamental substance [3]. It is a fascinating object to study because of its singular properties, because of its significance in biological systems, and because it is a classic example of hydrogen bonding [4]. Hydrogen bonding, which itself is one of the key elements in the functioning of life, is largely an electrostatic and polarization effect. Unfortunately, no commonly accepted model describes it simply and accurately at the same time. Here we show that the application of recent rules for minimal atomic multipoles [5] combined with the notion of distributed polarizabilities leads straightforwardly, without further intervention, to a very transparent model for electrostatic and polarization forces in water.

The intermolecular potential for water has been extensively studied, with about 150 models introduced since the 1930s, indicating difficulties in this area [6]. Recent accurate parametrizations involving several tens of parameters are available, based on tuning to rich vibration-rotation-tunneling (VRT) spectra [7,8], to high-level quantum-chemical calculations [9], or both [10]. Some models are based on molecular multipole moments and require high-order multipoles [11]. Following the seminal work by Rahman and Stillinger [12], many empirical models involve distributed charges [13–23]. Most of the force fields use static charges, thus ignoring or averaging polarization effects, while other models incorporate polarizabilities explicitly [16–23]. The work [17] first distributed the molecular polarizability over atomic sites.

It has recently been recognized that hydrogens need not be assigned charges in distributed-charge models [5]. The hydrogen's sole electron participates in the chemical bond and is not centered at the proton. Therefore, hydrogen is best described by an atomic dipole μ_H placed on the proton and directed along the bond. Assigning both a charge and a dipole causes redundancy and leads to unphysical results. This rule is an integral part of the minimal atomic multipole expansion (MAME) [5], which eliminates the redundancies by a careful choice of the minimal set of atomic multipoles, based on the Lewis structure of the molecule.

MAME rules lead to the following expression for the electrostatic potential of a single water molecule:

$$\phi(\mathbf{r}) = \mu_H \frac{(\mathbf{r}-\mathbf{r}_1)\cdot\mathbf{r}_1/l}{|\mathbf{r}-\mathbf{r}_1|^3} + \mu_H \frac{(\mathbf{r}-\mathbf{r}_2)\cdot\mathbf{r}_2/l}{|\mathbf{r}-\mathbf{r}_2|^3} + \mu_O \frac{\mathbf{r}\cdot\mathbf{n}}{r^3} + \theta_O \frac{2r^2 - 3(\mathbf{r}\cdot\mathbf{n}_1)^2 - 3(\mathbf{r}\cdot\mathbf{n}_2)^2}{2r^5}. \quad (1)$$

Since protons have no charge, neutrality allows no charge on the oxygen either. The dipole μ_O and quadrupole θ_O describe the two lone pairs on the oxygen [5]. The origin is at the oxygen, $\mathbf{r}_{1,2}$ are the positions of the protons, $r_{1,2} = l$, $\mathbf{n} = (\mathbf{r}_1 + \mathbf{r}_2)/|\mathbf{r}_1 + \mathbf{r}_2|$ is the unit vector along the symmetry axis, and $\mathbf{n}_{1,2}$ are unit vectors in the directions of lone pairs (Fig. 1). The experimental geometry has $l = 0.9572$ Å and a nearly tetrahedral bond angle $\beta = 104.52°$

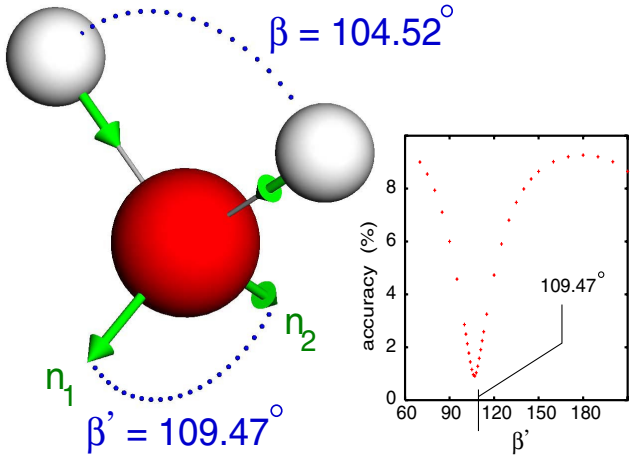

FIG. 1 (color online). Geometry of a single water molecule. Vectors $\mathbf{n}_1$ and $\mathbf{n}_2$ point in the direction of the lone pairs on the oxygen. The inset shows the effect of varying β' on the accuracy [5] of (1). μ_H, μ_O, and θ_O are reoptimized for every β'.

between $\mathbf{r}_1$ and $\mathbf{r}_2$ [24]. We take $\mathbf{n}_1$ and $\mathbf{n}_2$ to be at the tetrahedral angle $\beta' = 109.47°$ [19]. Significant deviation from this value leads to a dramatic deterioration of the accuracy of Eq. (1), as seen in the inset.

Our goal is to extend the static model to describe the field induced by a polarized molecule subject to external fields. In doing so we again keep only the minimal set of multipoles to avoid redundancies. The charge redistribution part of the molecular polarizability [25] ("FQ" or "fluctuating charge" is another name for the same concept [18]) vanishes for water due to the absence of charged sites. Thus we assign polarizabilities to individual nuclei in such a way as to reproduce the experimental molecular polarizability. The smallest component is $\alpha_{yy} = 1.4146(3)$ Å^3 normal to the molecular plane, the next is $\alpha_{zz} = 1.4679(13)$ Å^3 along the dipole moment, and the largest is $\alpha_{xx} = 1.5284(13)$ Å^3 in the longest dimension [26].

Atomic polarizabilities reflect the local atomic environments and need not necessarily be isotropic. The tetrahedral coordination of oxygen suggests assigning it an isotropic polarizability α_O. For hydrogens the polarizability α_H along the OH bond may differ from the polarizability $\alpha_\perp$ normal to it. To deduce α_O, α_H, and $\alpha_\perp$ we use them to express the molecular polarizability,

$$\begin{aligned}\alpha_{xx} &= \alpha_O + 2\alpha_H \sin^2\beta/2 + 2\alpha_\perp \cos^2\beta/2,\\ \alpha_{yy} &= \alpha_O + 2\alpha_\perp,\\ \alpha_{zz} &= \alpha_O + 2\alpha_H \cos^2\beta/2 + 2\alpha_\perp \sin^2\beta/2.\end{aligned} \tag{2}$$

In a surprise twist, the determinant of this linear system is identically zero. Equations (2) are therefore dependent and possess a solution only if the quantity

$$\alpha_{xx}\cos^2\beta/2 + \alpha_{yy}(2\sin^2\beta/2 - 1) - \alpha_{zz}\sin^2\beta/2 \tag{3}$$

is zero. Thus, the model is adequate if the above relation holds between the molecular polarizability components. Substituting the experimental values into (3) we get 0.0093 Å^3, which is indeed close to zero. Two independent equations suggest that one of the atomic polarizabilities can be safely omitted. The natural choice is to set $\alpha_\perp = 0$, implying that the dipole moments on protons can change their value, but not direction. Solving (2) we get

$$\begin{aligned}\alpha_O &= \alpha_{yy} = 1.4146 \text{ Å}^3,\\ \alpha_H &= (\alpha_{xx} + \alpha_{zz})/2 - \alpha_{yy} = 0.0836 \text{ Å}^3.\end{aligned} \tag{4}$$

Thus, the bulk of molecular polarizability comes from the oxygen, which is consistent with its atomic size, while the small polarizabilities on the protons account for the (small) anisotropy of the molecular polarizability tensor.

Three gas-phase multipoles from a density functional calculation, $\mu_H = 0.675$ D, $\mu_O = 1.033$ D, and $\Theta_O = 1.260$ D Å [5] result in the molecular dipole $\mu = 1.854$ D and the quadrupole components $\Theta = \Theta_{xx} - \Theta_{yy} = 4.973$ D Å and $\Theta_{zz} = 0.142$ D Å [27]. These should be compared to the experimental values [28,29] $\mu = 1.8546(6)$ D, $\Theta = 5.126(25)$ D Å, and $\Theta_{zz} = 0.113(27)$ D Å.

We again adjust the three atomic multipoles to satisfy the three experimental values precisely to avoid any computational input. The molecular dipole and quadrupole are expressed in terms of the atomic multipoles as

$$\begin{aligned}\mu &= \mu_O + 2\mu_H \cos\beta/2,\\ \Theta &= 6l\mu_H \sin^2\beta/2 + 3\theta_O \sin^2\beta'/2,\\ \Theta_{zz} &= 2l\mu_H(3\cos^2\beta/2 - 1) - \theta_O(3\cos^2\beta'/2 - 1).\end{aligned} \tag{5}$$

In practice, we face here an almost identical problem, in that the determinant of (5) is small. It becomes zero when the ideal tetrahedral angle is substituted for β. A relation similar to (3) in this case reads simply $\Theta_{zz} = 0$. Actual Θ_{zz} is indeed small, but not zero, and β deviates noticeably from 109.47°. Nevertheless, the smallness of the determinant indicates that the data, which have finite accuracy, can be satisfied by a range of atomic multipoles, and so the third equation in (5) cannot be used reliably.

Thus, we use the first two equations to express μ_O and θ_O in terms of μ_H, which guarantees the experimental μ and Θ are reproduced while keeping reasonable Θ_{zz}. The density functional theory value $\mu_H = 0.675$ D yields $\mu_O = 1.029$ D and $\theta_O = 1.352$ D Å, with $\Theta_{zz} = 0.160$ D Å. The model is thus completely defined and readily yields the Coulomb and induction energy E_P for the water dimer, trimer, and larger clusters [25].

Water clusters from dimers on up have been extensively studied with both experiment [7,30–32] and theory [7,8,33–35]. The six-dimensional adiabatic energy surface

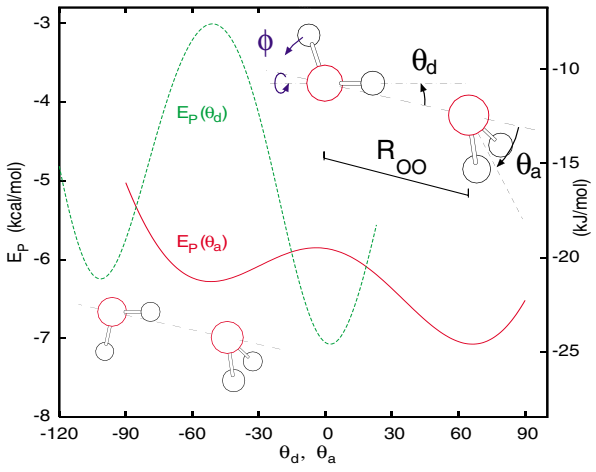

FIG. 2 (color online). Coulomb + induction energy $E_P(\theta_a, \theta_d)$ for the water dimer. $R_{OO} = 2.977$ Å, and one of the angles is fixed at the minimum value as the other one is varied. E_P is calculated for the defined system of atomic multipoles and polarizabilities in the standard manner [25], by computing the fields of all multipoles of one molecule exerted on the multipoles of another molecule, and solving for self-consistency.

of the dimer has eight equivalent minima [36] split in a complex fashion by zero-point tunneling motion. The softness of the pair potential requires care when relating it to experimental observables [7].

The equilibrium hydrogen-bonded configuration has a symmetry plane (Fig. 2, inset) and is characterized by the oxygen-oxygen distance R_{OO}, the donor angle θ_d, and the acceptor angle θ_a. The hydrogen bond forms when the donor proton points against one of the lone pairs of the acceptor, $\theta_d \approx 0$, $\theta_a \approx \beta'/2 = 54.74°$ in our notation. The actual angles deviate slightly from these ideal values and are known with some scatter.

For the experimental geometry we get $E_P = -7.046$ kcal/mol (-29.48 kJ/mol). Adding 1.820 kcal/mol for the exchange and dispersion energy [VRT(ASP-W)III [8] value] we get the equilibrium binding energy $D_e = 5.110$ kcal/mol (21.38 kJ/mol). The model also yields the total dipole moment of the dimer in excellent agreement with experiment (Table I). The induction contribution alone is about 20% of D_e and decreases with R_{OO}.

Since E_P is only a part of the total interaction, which also contains exchange and dispersion terms, we fix R_{OO} and analyze the orientation dependence (Fig. 2). The minimum is achieved at $\theta_d = 2.14°$ and $\theta_a = 66.26°$, which is close to, but should not be confused with, the equilibrium hydrogen-bonded configuration, since other terms may shift the minimum. Rotation of either the donor by $\Delta\theta_d \approx -\beta$ or the acceptor by $\Delta\theta_a \approx -\beta'$ produces an alternative hydrogen-bonded arrangement sketched under the local minima in Fig. 2.

In order to further assess the quality of the model, we analyze the energy variation along a path where the exchange and dispersion terms vary little. We chose to rotate the donor by an angle ϕ around the bridging OH bond (Fig. 2). Only a single proton then changes its position and stays far from all the nuclei of the acceptor for all ϕ.

Figure 3 shows excellent agreement with all three best pair potentials. Note the small (<1 kcal/mol) total amplitude of the variation, which is not described by a simple $\cos\phi$ function. The overall agreement in the full range of ϕ is better with the *ab-initio*-based SAPT-5S [9] potential (inset). However, at small ϕ we get a near coincidence with the other two curves, VRT(ASP-W)III and SAPT-5ST [10],

TABLE I. Equilibrium binding energy D_e (kcal/mol) and dipole moment $\mu^{\rm dim}$ (Debye) for water dimer. $\mu_\perp^{\rm dim}$ is the component of $\mu^{\rm dim}$ normal to the principal axis.

	R_{OO} (Å)	θ_d	θ_a	D_e	$\mu^{\rm dim}$	$\mu_\perp^{\rm dim}$
SAPT-5S	2.955	6.36°	52.83°	4.858		
SAPT-5ST	2.924	6.95°	58.52°	5.026		
VRT(ASP-W)III	2.947	1.86°	49.27°	4.948	2.69[b]	
This work[a]	2.977	0.74°	59.7°	5.110	2.67	0.13
Expt. [29,30]	2.977	0.74°	59.7°		2.67	0.38

[a]Geometry is fixed at experimental values.
[b]Projection on the principal axis [7].

which are both spectroscopically tuned. This is very encouraging, assuming the spectroscopic tuning is more sensitive to the region near the equilibrium.

The model also performs well for the displacement of the donor with respect to the acceptor (lower inset). For comparison, TIP4P-FQ, a popular polarizable model with fluctuating charges on the oxygen and hydrogens, gives softer E_P at small distances because it underestimates the molecular polarizability [18].

Explicit distributed polarizabilities (4) suggest an estimate of the dispersion energy. Because of the fast r^{-6} decay, the dispersion is dominated by two terms, $E^D_{OO} \propto \alpha_O\alpha_O$ and $E^D_{HO} \propto \alpha_H\alpha_O$. Small α_H in the second term is compensated by the proximity of the bridging hydrogen to the oxygen of the acceptor. Neglecting dispersion nonadditivity and assuming a universal scaling of the dispersion coefficient $C_6 \approx z\alpha_A\alpha_B$ for A and B species, we get $E^D_{OO} = z\alpha_O^2/R^6_{OO} = 0.99$ kcal/mol and $E^D_{HO} = \frac{2}{3}z\alpha_H\alpha_O/(R_{OO} - l)^6 = 0.40$ kcal/mol for a linear hydrogen bond. The total $E^D = 1.39$ kcal/mol (5.82 kJ/mol) can be compared to 1.56 kcal/mol from Fig. 3 of Ref. [35]. For this crude estimate we used $z = 344$ kcal/mol value for Ar. The factor of $\frac{2}{3}$ accounts for the anisotropy of α_H [37].

Since our model is constructed based solely on monomer properties, we may speculate that it should describe larger clusters as well, where the nonpairwise additivity of energy

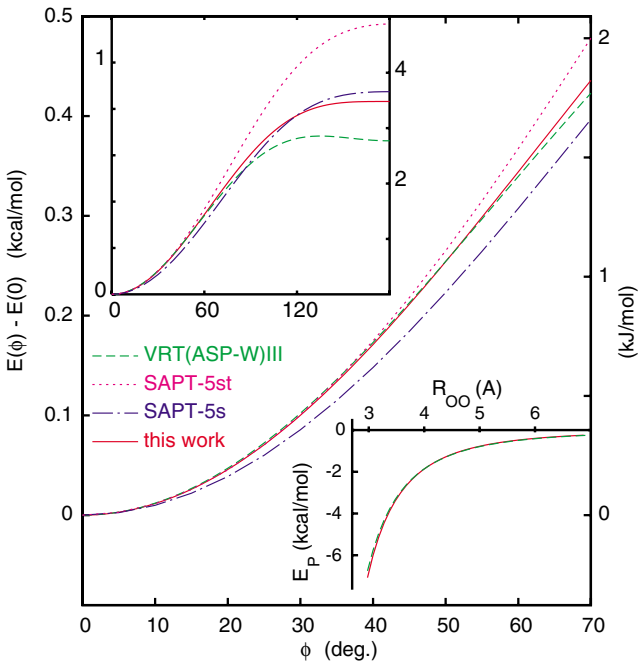

FIG. 3 (color online). Energy variation for the water dimer with rotation of the donor around the bridging OH bond. The agreement is best with the spectroscopically tuned potentials at small ϕ and with the *ab-initio*-based potential overall. The lower inset compares E_P with the Coulomb + induction part of the VRT(ASP-W)III potential over the donor-acceptor separation along the O–O line (experimental geometry used).

is important [9,31]. Such nonadditivity results from self-consistency of all the induced moments in the cluster [25], and may be relevant for the cooperativity of hydrogen bonding in protein secondary structures [38].

It is interesting to apply the present model to larger clusters and to liquid water, where recent studies employ polarizable force fields [39–41]. This requires a suitable parametrization of the exchange repulsion and dispersion terms. It is particularly appealing to augment the model with fine-tuning of the repulsion terms to reproduce VRT spectroscopic features [7].

The MAME approach used here bears similarities with the works of Stone and others [42–44]. The difference is that here no attempt is made to reproduce the electronic density by partitioning the molecular volume into regions or ''basins.'' The MAME multipoles are not designed to be the multipole moments of these regions, but merely to reproduce the electrostatic potential of the molecule as a whole. This allows for freedom in the choice of the minimal multipole set that eliminates redundancies [5].

For larger molecules experimental data will not be sufficient to deduce atomic multipoles and polarizabilities, and the multipoles from the MAME calculation may have to be used [5]. These values for water are close to those deduced from experiment, which is encouraging.

The author is grateful to M. Pederson and G. Scoles for enlightening conversations. He also appreciates the VRT-III computer program provided by R. J. Saykally and N. Goldman. Numerous discussions with A. Shabaev, Al. L. Efros, and J. Feldman and help with 3D graphics by N. Bernstein are kindly acknowledged. This work was supported by the Office of Naval Research.

*Electronic address: etsiper@gmu.edu

[1] C. A. Coulson and D. Eisenberg, Proc. R. Soc. London A **291**, 445 (1966).
[2] B. Chen, I. Ivanov, M. L. Klein, and M. Parrinello, Phys. Rev. Lett. **91**, 215503 (2003).
[3] Genesis 1:1–2.
[4] S. Scheiner, *Hydrogen Bonding. A Theoretical Perspective* (Oxford University Press, Oxford, 1997).
[5] E. V. Tsiper and K. Burke, J. Chem. Phys. **120**, 1153 (2004).
[6] *Water: Structure, State, Solvation. Recent Achievements* (in Russian), edited by A. M. Kutepov (Science, Moscow, 2003).
[7] R. S. Fellers, C. Leforestier, L. B. Braly, M. G. Brown, and R. J. Saykally, Science **284**, 945 (1999).
[8] N. Goldman *et al.*, J. Chem. Phys. **116**, 10 148 (2002).
[9] G. C. Groenenboom, E. M. Mas, R. Bukowski, K. Szalewicz, P. E. S. Wormer, and A. van der Avoird, Phys. Rev. Lett. **84**, 4072 (2000).
[10] G. C. Groenenboom *et al.*, J. Chem. Phys. **113**, 6702 (2000).
[11] E. R. Batista *et al.*, J. Chem. Phys. **112**, 3285 (2000).
[12] A. Rahman and F. H. Stillinger, J. Chem. Phys. **55**, 3336 (1971).
[13] J. L. Finney, J. Mol. Liq. **90**, 303 (2001).
[14] H. J. C. Berendsen, J. P. M. Postma, W. F. van Gunsteren, and J. Hermans, in *Intermolecular Forces*, edited by B. Pullman (Reidel, Dordrecht, 1981), p. 331.
[15] M. W. Mahoney and W. L. Jorgensen, J. Chem. Phys. **112**, 8910 (2000).
[16] J. Caldwell, L. X. Dang, and P. A. Kollman, J. Am. Chem. Soc. **112**, 9144 (1990).
[17] D. N. Bernardo, Y. Ding, K. Krogh-Jespersen, and R. M. Levy, J. Phys. Chem. **98**, 4180 (1994).
[18] S. W. Rick *et al.*, J. Chem. Phys. **101**, 6141 (1994).
[19] H. A. Stern *et al.*, J. Chem. Phys. **115**, 2237 (2001).
[20] G. Lamoureux *et al.*, J. Chem. Phys. **119**, 5185 (2003).
[21] P. Ren and J. W. Ponder, J. Phys. Chem. B **107**, 5933 (2003).
[22] H. B. Yu *et al.*, J. Chem. Phys. **118**, 221 (2003).
[23] I. M. Svishchev *et al.*, J. Chem. Phys. **105**, 4742 (1996).
[24] W. S. Benedict *et al.*, J. Chem. Phys. **24**, 1139 (1956).
[25] E. V. Tsiper and Z. G. Soos, Phys. Rev. B **64**, 195124 (2001).
[26] W. F. Murphy, J. Chem. Phys. **67**, 5877 (1977).
[27] B3LYP/aug-cc-pVTZ hybrid density functional calculation yields geometry $l = 0.9619$ Å and $\beta = 105.08°$, using the GAUSSIAN 98 program by M. J. Frisch *et al.* (Gaussian Inc., Pittsburgh, 1995).
[28] S. A. Clough *et al.*, J. Chem. Phys. **59**, 2254 (1973).
[29] J. Verhoeven and A. Dymanus, J. Chem. Phys. **52**, 3222 (1970). The value Q_{zz} depends on the choice of the origin of coordinates, and is cited here relative to the oxygen.
[30] J. A. Odutola and T. R. Dyke, J. Chem. Phys. **72**, 5062 (1980).
[31] N. Pugliano and R. J. Saykally, Science **257**, 1937 (1992).
[32] L. A. Curtiss *et al.*, J. Chem. Phys. **71**, 2703 (1979).
[33] O. Matsuoka, E. Clementi, and M. Yoshimine, J. Chem. Phys. **64**, 1351 (1976).
[34] C. Millot, J.-C. Soetens, M. T. C. M. Costa, M. P. Hodges, and A. J. Stone, J. Phys. Chem. A **102**, 754 (1998).
[35] X. Wu, M. C. Vargas, S. Nayak, V. Lotrich, and G. Scoles, J. Chem. Phys. **115**, 8748 (2001).
[36] B. J. Smith, D. J. Swanton, J. A. Pople, H. F. Schaefer III, and L. Radom, J. Chem. Phys. **92**, 1240 (1990).
[37] The second-order perturbation expression for C_6 contains the combination $\mu_{1x}^2\mu_{2x}^2 + \mu_{1y}^2\mu_{2y}^2 + 4\mu_{1z}^2\mu_{2z}^2$ of the transition dipole matrix elements (here z is along the line connecting the atoms). For two isotropic atoms this gives a numerical factor of 6, whereas setting the x and y components to zero for anisotropic α_{H} reduces this factor to 4. The reduction factor is, therefore, $\frac{2}{3}$.
[38] J. Ireta *et al.*, J. Phys. Chem. B **107**, 1432 (2003).
[39] B. Chen, J. H. Xing, and J. I. Siepmann, J. Phys. Chem. B **104**, 2391 (2000).
[40] S. W. Rick, J. Chem. Phys. **114**, 2276 (2001).
[41] G. Hura *et al.*, Phys. Chem. Chem. Phys. **5**, 1981 (2003).
[42] A. J. Stone, *The Theory of Intermolecular Forces* (Clarendon Press, Oxford, 1996).
[43] G. Jansen *et al.*, Mol. Phys. **88**, 69 (1996); **91**, 145 (1997).
[44] R. F. W. Bader, *Atoms in Molecules—A Quantum Theory* (Oxford University Press, Oxford, 1990).